Electromagnetic Excitation Technique for Nonlinear Resonant Ultrasound Spectroscopy

Joshua F Gregg

A senior thesis submitted to the faculty of
Brigham Young University
in partial fulfillment of the requirements for the degree of

Bachelor of Science

Brian E. Anderson, Advisor

Department of Physics and Astronomy

Brigham Young University

ABSTRACT

Electromagnetic Excitation Technique for Nonlinear Resonant Ultrasound Spectroscopy

Joshua F Gregg
Department of Physics and Astronomy, BYU
Bachelor of Science

Nonlinear resonant ultrasound spectroscopy (NRUS) is a method that can be used for detecting the amount of microcracking in structures. NRUS detects global damage in a sample by measuring shifts in resonance frequencies that depend on excitation amplitude and correspond to nonlinear elastic properties of the material. NRUS measurements typically are excited with a piezoelectric transducer, but here the application of an electromagnetic transducer is explored as an alternative. The electromagnetic transducer, unlike a single piezoelectric, allows selective excitation of longitudinal, torsional, and bending vibrations in a rod-shaped sample. Measurement of the nonlinear properties of the sample for each type of vibration is therefore possible. This electromagnetic technique involves gluing a coil of wire onto the end of a rod sample and placing it in a magnetic field. By controlling which part of the coil is inside the strongest region of the magnetic field, the principle direction of the driven oscillations in the rod can be controlled. Both piezoelectric and electromagnetic excitation techniques are tested by measuring the nonlinear elastic parameter, α_E, of Berea sandstone. The electromagnetic technique was shown to measure a 30% higher mean value for α_E than the piezoelectric technique.

Keywords: NRUS, NDE, nonlinear acoustics, elasticity, resonance

ACKNOWLEDGMENTS

This research was done with funding from the Brigham Young University College of Physical and Mathematical Sciences. The author wishes to thank Brian Anderson for his years of instruction and guidance, Marcel C. Remillieux for advice on NRUS experimental practices, and Pierre-Yves Le Bas of Los Alamos National Laboratory for licensing the Resonance Inspection Techniques and Analysis (RITA) software, which he wrote, with BYU.

Contents

List of Figures

Chapter 1

Introduction

Nonlinear resonant ultrasound spectroscopy (NRUS) is a method used to measure nonlinearities caused by cracks and grain boundary effects by observing the acoustic resonance frequencies of a sample under test [1, 2]. NRUS may be used for global nondestructive evaluation of materials, meaning the detection of the cumulative amount of damage in a sample, rather than to detect individual cracks [2]. The main advantage of NRUS over other nondestructive evaluation techniques is that it can detect the presence of microscopic cracks and grain boundary effects that other techniques relying on linear elasticity might not detect [3, 4]. For example, NRUS was recently used to detect stress corrosion cracking in steel [5]. It has also been used to measure fluid saturation levels in sandstone, which could help determine the presence of water or oil underground [6]. Cracks and grain boundary effects typically cause materials to soften and the resonance frequencies therefore typically shift downward with increasing vibration amplitude [2, 7].

NRUS was developed in the 1990's and its name was coined by Guyer and Johnson in 1999 [1,2]. A patent was granted in 2001 to Johnson *et al.*, who used a piezoelectric transducer made of lead zirconate titanate (PZT) to excite vibrations in their sample [8]. In 1996, Johnson *et al.* discovered a complication where the nonlinearity depends on the rate of the frequency sweep, because high-amplitude vibrations condition the sample and it takes time to recover to a linear state [9]. This

behavior was called "slow dynamics" [2]. To find out the severity of this complication, Pasqualini *et al.* made measurements at different strain amplitudes and determined that for strains below about 5×10^{-7}, slow dynamics were not noticeable, but above strains of around 10^{-6} they began to dominate [2, 10].

As these papers show, typically piezoelectric transducers made of lead zirconate titanate (PZT) are used to excite vibrations for NRUS measurements, in a configuration that can only excite one type of vibration. The inability of a single PZT transducer to excite multiple types of vibration modes is a disadvantage [11]. Garrett developed an electromagnetic excitation technique (hereafter referred to as the EM technique) that can selectively excite longitudinal, torsional, and bending vibrations in the same sample without the need to replace the transducer [12]. He used this technique for resonant ultrasound spectroscopy (RUS), a linear elastic technique used to extract the moduli of the elastic tensor, but it has never been used for NRUS. The EM transducer consists of a coil of wire carrying an alternating current, glued onto the end of a rod sample, with a portion of the coil placed in a magnetic field [12]. The EM excitation technique uses the Lorentz force exerted on a current-carrying coil of wire to excite vibrations in the sample. It allows direct excitation of longitudinal, bending, and torsional vibrations with just one transducer on the sample, by simply changing the orientation of the coil on the sample relative to the magnet. By controlling which part of the coil is in the strongest part of the magnetic field, the direction of the force applied to the end of the rod may be controlled. One possible disadvantage of this technique found in the current research is that the coil generates heat when current is running through it, and it in turn heats up the sample, which may change its elastic properties [3]. The EM technique could be considered a non-contact technique because the magnet does not need to touch the coil to excite the vibrations. Non-contact excitation techniques are desirable for NRUS because they make it possible to test materials quickly, over large areas [13]. There have been other non-contact excitation techniques developed, but none have been used for NRUS. Various types of air-coupled transducers

were reviewed in an article by Remillieux [13]. Some examples include: PZT transducers [14], capacitive ultrasonic transducers [15–17], laser-based thermoelastic sources [18], time reversal acoustic focusing [19], focused electric spark sources [20], and array techniques [12, 21]. These types of non-contact sources likely haven't been used for NRUS because they typically cannot generate high enough vibration amplitudes in samples, so the EM excitation technique is of interest as a more practical, quasi non-contact method of excitation [13].

There are three principal types of vibrational modes for a rod: longitudinal, torsional, and bending [22–25]. These different vibration modes are governed by different elastic restoring forces within the material. Linear longitudinal vibrational modes are governed by the Young's modulus. Linear torsional vibrational modes are governed by the shear modulus. Linear bending vibrational modes involve both moduli, in the general sense [26]. Remillieux *et al.* used a compressional mode PZT transducer to excite longitudinal vibrations for NRUS studies [11]. They also showed that it is possible to excite torsional vibrations using shear mode PZT transducers [11], but that method required gluing multiple shear mode PZT transducers around the end of the rod. Remillieux *et al.* showed, for the first time, that shifts in longitudinal and torsional mode frequencies are governed by two independent nonlinear elastic parameters, α_E and α_G, respectively.

The results presented here are limited to an analysis of the first longitudinal vibration mode. This is because the purpose of this research was to compare the EM excitation technique to the PZT excitation technique. Since the PZT technique is most convenient for longitudinal vibrations, the study was limited accordingly. Berea sandstone is used as the sample material because it exhibits high amounts of resonance peak shifting, and it has well known elastic properties [11, 27].

In the following chapters, the EM excitation technique, including the orientations needed to excite longitudinal, torsional, and bending vibrations, will be described. The results of individual measurements and of repeatability tests between the EM technique and the PZT technique will also be given. Extracted α_E parameters from each excitation technique will be compared to quantify

absolute errors between the techniques and random errors for each technique. Conclusions about the EM technique and its usefulness, in comparison to using a PZT technique, will then be given.

Chapter 2

Methods

2.1 Piezoelectric transducer

Past work with NRUS has been done almost exclusively with piezoelectric transducers made of lead zirconate titanate (PZT) to excite the vibrations in the sample. A PZT transducer is glued onto the end of a rod to excite longitudinal vibrations, and is assumed not to introduce any nonlinear effects in the vibrations. Fig. 2.1 shows a typical measurement configuration, with a sample of Berea sandstone. The PZT transducer is attached at the right end, and a laser Doppler vibrometer measures the sample's response at the left end. The sample is supported by rubber bands to approximate a free-free bar. Custom LabVIEW software was developed at Los Alamos National Laboratory and licensed to BYU to conduct NRUS measurements. During an NRUS measurement, the transducer is excited by stepping through a range of frequencies encompassing the resonance frequency, with a step size of 1Hz. The data acquisition software waits for a 100 ms ring-up time at each frequency before recording for 100 ms to measure the vibration amplitude. This is repeated at each frequency, producing a resonance curve. The frequency sweep is then repeated various times with a higher excitation amplitude each time, to produce several resonance curves (Fig. 2.2). Changing room

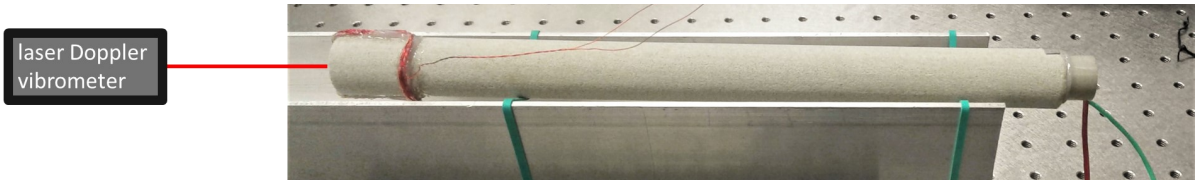

Figure 2.1 A PZT transducer exciting longitudinal vibrations in a rod sample, while a laser Doppler vibrometer measures the vibrations.

conditions like temperature can shift the resonance frequency during the measurement, so to reduce error from room effects, the lowest-amplitude resonance curve is measured over again after each higher-amplitude resonance curve, and the frequency shift of each peak relative to its corresponding low-amplitude peak is measured. This method was introduced by Haupert *et al.* [3]. For the examples in Fig. 2.2, the low-amplitude peak shifts in frequency by 6 Hz over the course of the measurement for the PZT excitation example, and by 1 Hz for the EM excitation example.

The equipment used for these experiments is as follows: The PZT transducer is a cylindrical, APC International, type 850 PZT, measuring 19mm in diameter and 12mm thick. It is bonded to the sample with 5-minute epoxy. The signal for the transducer is generated by a National Instruments PXI-5406 generator card and amplified by a Tabor Electronics 9400 amplifier that is capable of producing a signal of up to 200 V amplitude. The voltage amplitudes used to generate Fig. 2.2(a) ranged from 30V to 150V in steps of 20 V. To measure the vibrations, a Polytec PSV-400 scanning laser Doppler vibrometer was used, with the laser reflecting off patches of retro-reflective tape applied to the surface of the sample. The laser vibrometer was connected to a National Instruments PXIe-5122 14-Bit digitizer card. The sandstone sample is a cylindrical Berea sandstone core from Cleveland Quarries in Vermilion, OH, and measures 2.54 cm in diameter and 30.48 cm in length. The permeability to air for this core is 500 millidarcys.

After an NRUS measurement has been done for a sample (Fig. 2.2), the velocity amplitude at

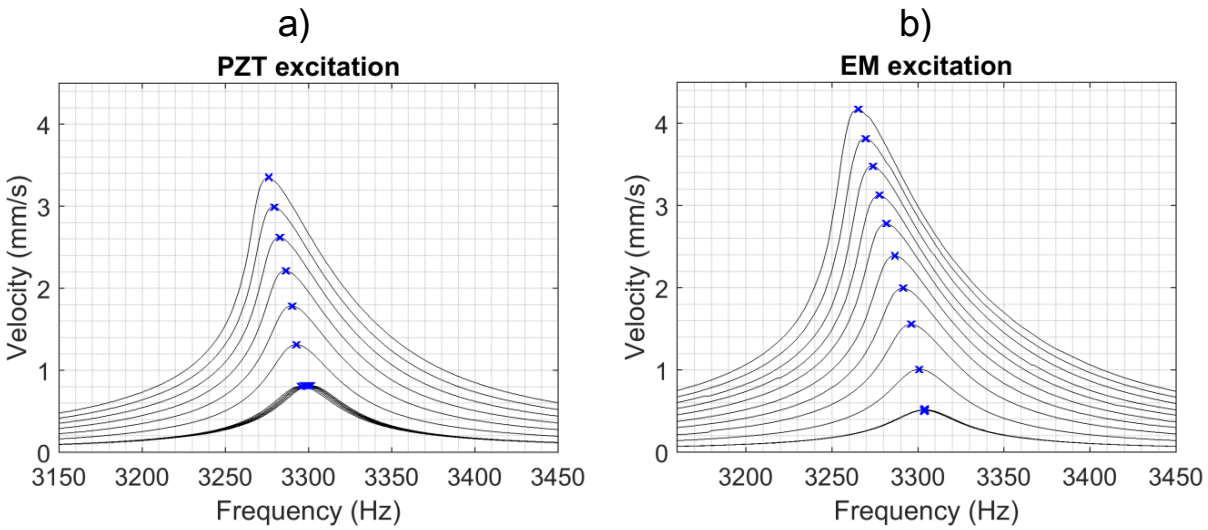

Figure 2.2 NRUS measurements using (a) PZT excitation and (b) EM excitation. The lowest-amplitude resonance curve is repeated after each higher-amplitude curve. The blue markers represent f_n and v_{max} for each peak.

each peak frequency, v_{max}, is used to calculate the strain at the peaks, using the formula

$$\varepsilon_{max} = v_{max}/c. \tag{2.1}$$

For example, the highest peak in Fig. 2.2(a) has $v_{max} = 3.35\,\text{mm/s}$, which corresponds to a peak strain of 1.66×10^{-6}. In Eq. (2.1), c is the longitudinal sound speed in the material. For the sandstone sample, $c = 2013\,\text{m/s}$, which is calculated using $c = f_{0avg}(2L_{sample})$ where L_{sample} is the length of the sample and f_{0avg} is the average frequency of all the low-amplitude peaks . The relative frequency shift of each peak, Δf, is calculated as

$$(f_{0n} - f_n)/f_{0avg} = \Delta f, \tag{2.2}$$

where f_{0n} is the frequency of the low-amplitude reference peak corresponding to the n^{th} amplitude peak and f_n is the frequency of the n^{th} amplitude peak. Note that the higher-amplitude peaks are shifted down in frequency, but Δf from Eq. (2.2) is defined such that it gives a positive number, to indicate the magnitude of the frequency shift. As an example of these computations, in Fig. 2.2(a),

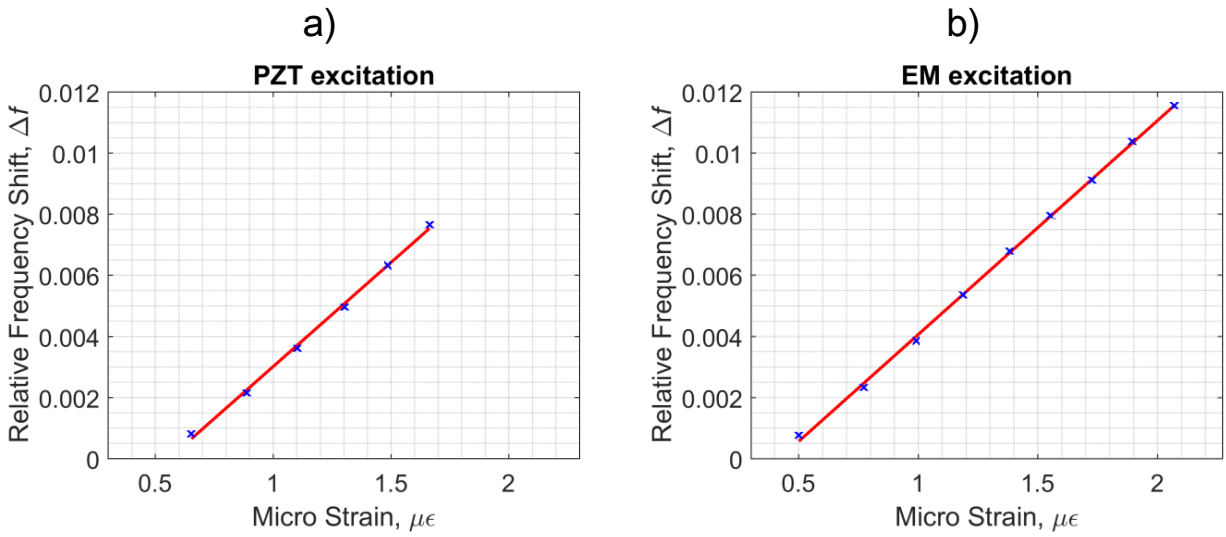

Figure 2.3 Example of linear fits to find the nonlinearity parameter α_E for NRUS measurements done with (a) PZT excitation, and (b) EM excitation. α_E is the slope of the line made by plotting relative frequency shift as a function of strain.

$f_6 = 3276.16\,\text{Hz}$ is the frequency of the highest peak ($n = 6$), $f_{06} = 3301.45\,\text{Hz}$ is the frequency of its corresponding low-amplitude peak, $f_{0avg} = 3298.7\,\text{Hz}$ is the low-amplitude average frequency, and $\Delta f = 0.77\%$ is the relative frequency shift. The nonlinearity parameter α_E is calculated by plotting the relative frequency shift of each peak against the peak strain amplitude (Fig. 2.3). A linear fit is applied to this data, and the slope of the line is α_E. In Fig. 2.3(a), the value calculated for α_E is 7800 with correlation coefficient $R = 99.9\%$. This parameter tells how the material's Young's modulus depends on strain amplitude, following the relationship [11]

$$E = E_0(1 - \alpha_E \varepsilon_{max}). \tag{2.3}$$

2.2 Electromagnetic transducer

The EM transducer is a coil of wire glued onto the sample with 5-minute epoxy and placed in a magnetic field. By running an alternating current through the coil, vibrations in the sample

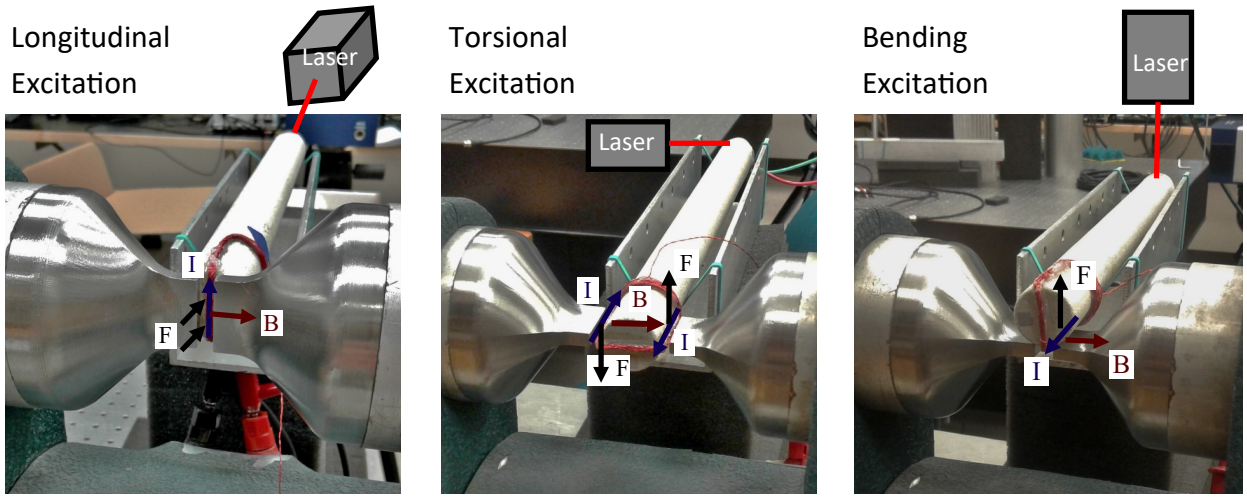

Figure 2.4 Configurations for exciting longitudinal, torsional, and bending vibrations with a coil in a magnetic field. The driving force is the Lorentz Force, $\vec{F} = I\vec{L} \times \vec{B}$, where $\vec{F}$ is force, I is current, $\vec{L}$ is a vector pointing along the length of wire, and $\vec{B}$ is magnetic field.

are excited with the Lorentz force. By changing the orientation of the coil in the magnetic field, longitudinal, torsional, and bending vibrations may be excited without having to use multiple transducers. Fig. 2.4 shows the configurations for each type of vibration excitation. Being able to excite all three types of vibrations allows a study of elastic nonlinearities for both compressional and shear waves.

The magnet is an electromagnet, capable of producing a field up to 0.25 T between the poles. Fig. 2.5 is a photograph of the magnet with its power supply. During an NRUS measurements using the EM excitation technique, the power supply provides 51.8 V and 2.1 A to the electromagnet. The magnet pole pieces were designed to concentrate the magnetic field over a small area, and they were made of 416 stainless steel because of its machinability, high corrosion resistance, and relatively high magnetic permeability. To drive the coil transducer, a Crown XLS 202 audio amplifier is used with a series 4 Ω current-limiting resistor, rated for 100W of power. The coil itself is 3 m of 30 gauge copper magnet wire, wound into 21 turns, and has 1 Ω of resistance. The voltage amplitudes across the coil ranged from 0.17 V to 1.7 V in steps of 0.17 V.

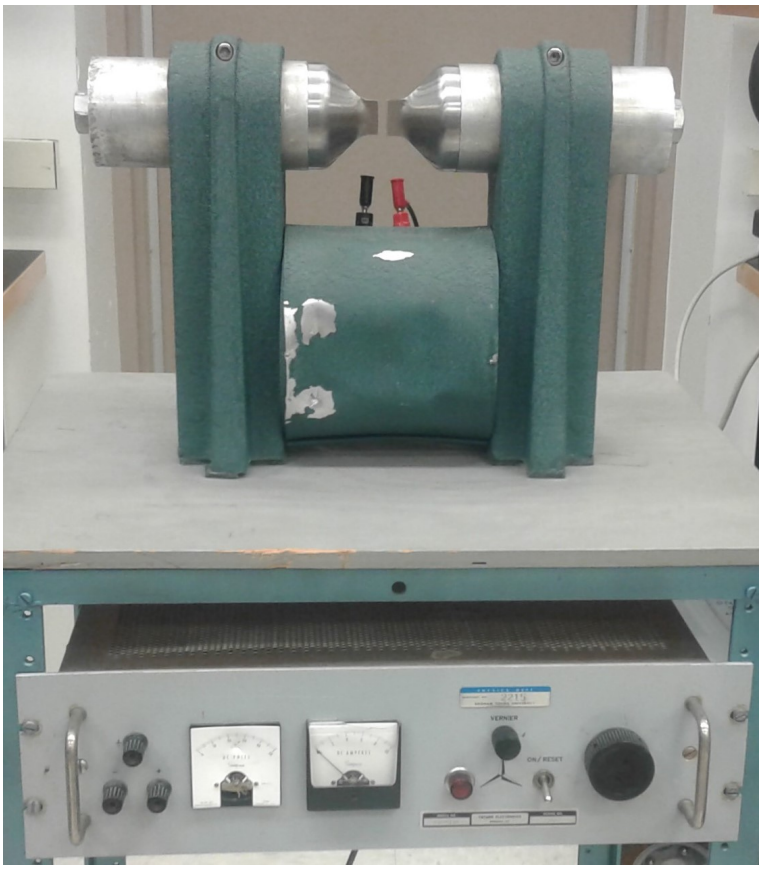

Figure 2.5 Photograph of the electromagnet used for the EM excitation technique, with its power supply.

It was found that the EM excitation technique can excite several resonances in the Berea sandstone sample for longitudinal, torsional, and bending vibrations, and shows little unwanted coupling between vibration types. For the Berea sandstone sample, the technique was able to excite at least the first four resonance modes for each type, with only small contributions from modes of the other types. The frequency response was measured for each type of vibration between 0-20 kHz (Fig. 2.6) to demonstrate the capability of the EM technique. In the figure, the first few resonance peaks are clearly visible for each type of vibration and are identified by added vertical lines. This means that the EM excitation technique will be capable of doing NRUS measurements for all three types of vibration.

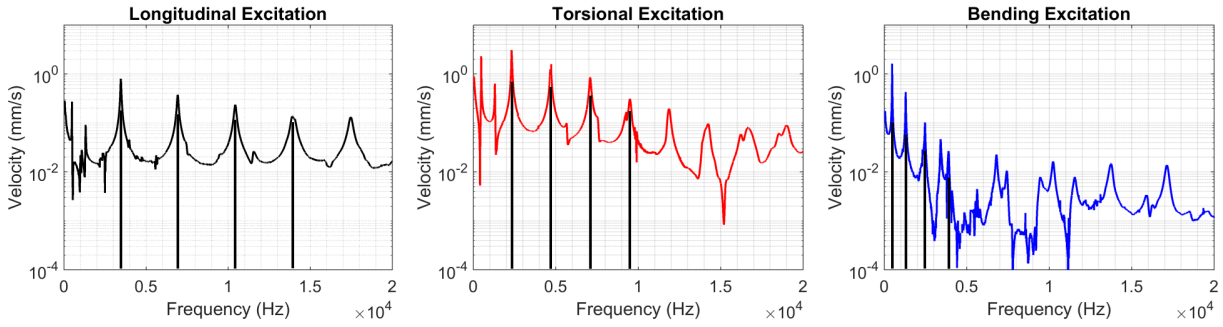

Figure 2.6 Frequency response curves of a sandstone sample as a demonstration of the EM excitation technique for longitudinal, torsional, and bending vibrations. The resonance frequencies are highlighted by vertical lines, and at least the first few modes are clearly visible for each vibration type.

To do an NRUS measurement with the EM excitation technique, the process is similar to the PZT excitation technique. The coil of magnet wire is glued onto the end of a rod and the sample and magnet are positioned in the configuration that excites longitudinal vibrations (Fig. 2.4). The coil transducer steps through the same range of frequencies as before, in steps of 2 Hz. The sample's response is again measured with the laser Doppler vibrometer, and the data acquisition software waits for the 100 ms ring-up time before recording for 50 ms at each frequency. This is repeated at different amplitudes to get the NRUS peaks. In Fig. 2.2(b), the highest peak ($n = 9$) has $v_{max} = 4.17\,\text{mm/s}$, and using Eq. (2.1) with $c = 2015\,\text{m/s}$, this corresponds to a peak strain of 2.07×10^{-6}. The frequency of this peak is $f_9 = 3265.27\,\text{Hz}$, the frequency of its corresponding low-amplitude peak is $f_{09} = 3303.46\,\text{Hz}$, and $\Delta f = 1.16\%$ is the relative frequency shift, where the low-amplitude average frequency is $f_{0avg} = 3304\,\text{Hz}$. The parameter α_E is calculated in the same manner as before. Fig. 2.3(b) shows the linear fit used to compute α_E, and the value for this particular measurement was 7000, with correlation coefficient $R = 99.96\%$. Note that for the equipment used in this work, the EM excitation technique was capable of generating slightly higher strains than PZT excitation. With the PZT technique, the maximum strain is limited by the voltage range of the amplifier, while with the EM technique it is limited by the current limit of the coil and

the magnetic field strength.

Chapter 3

Results

In the examples given in Chapter 2, the EM technique yielded a different value of α_E from the PZT technique. Since the purpose of this work is to compare results of the EM technique to the PZT technique, it became important to know whether the discrepancy is due to absolute error caused by differences between the techniques, or random error. Repeatability tests were conducted to determine the amounts of absolute and random error in both techniques, which included back-to-back NRUS measurements with no time between them, as well as NRUS measurements taken on different days. These tests showed that back-to-back measurements are much more consistent than measurements taken on different days. The EM excitation technique consistently yields higher values of α_E than the PZT excitation technique. Heat generated by the coil during EM excitation was examined as a possible cause of the absolute error, but it was concluded that it was not the cause. As for the random error, correlation between α_E and room conditions like temperature and humidity were examined, and it was found that α_E for the Berea sandstone sample correlates highly with humidity, while α_E for a steel sample correlates with temperature. This chapter will now present these findings.

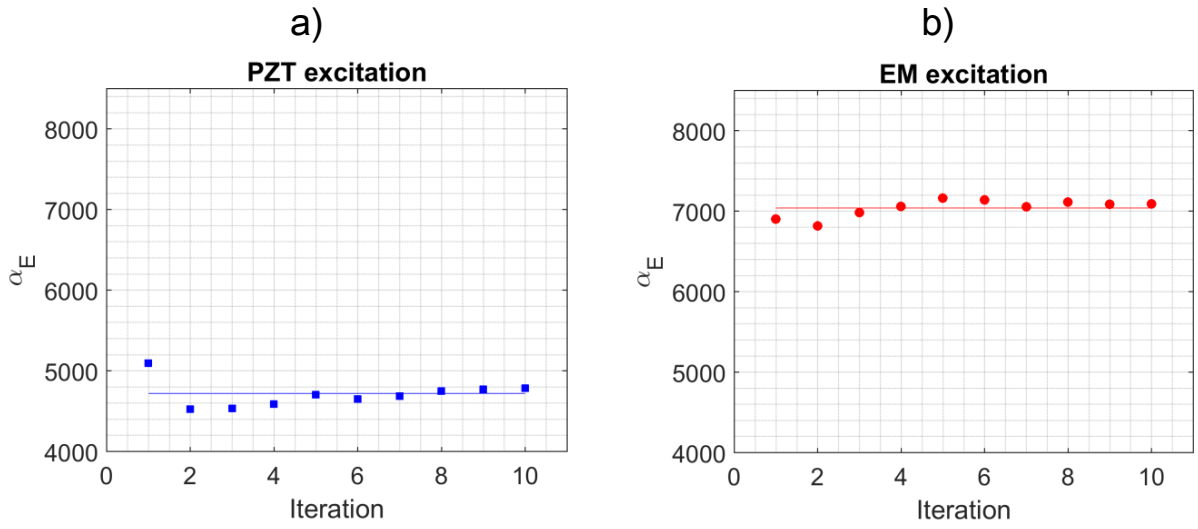

Figure 3.1 Values of the nonlinearity parameter, α_E, for 10 back-to-back NRUS measurements using (a) PZT excitation, and (b) EM excitation. The solid lines represent mean values.

3.1 Back-to-back NRUS measurements

Each set of back-to-back measurements consisted of 10 full NRUS measurements with the same transducer each time, and each successive measurement starting directly after the previous one ends. For clarity, one full NRUS measurement consists of multiple resonance curves at different excitation amplitudes, from which an α_E value is extracted. Values of α_E for one such set of measurements using the PZT transducer are shown in Fig. 3.1(a). The mean of these α_E values is 4720, and the relative standard deviation (RSTD) is 3.4% (note that RSTD is the standard deviation divided by the mean).

For a similar set of measurements using the EM transducer, the mean α_E was 7040 and the RSTD was 1.6%. Fig. 3.1(b) shows the back-to-back NRUS measurements using the EM technique. Note that back-to-back NRUS measurements showed relatively consistent α_E values, and that the EM technique gives higher values of α than the PZT technique, which turned out to be a general trend.

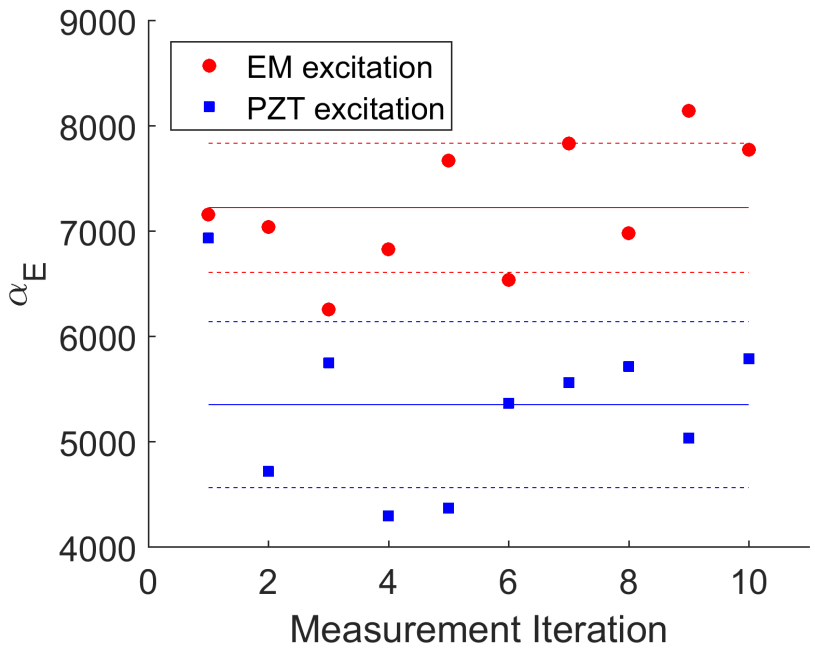

Figure 3.2 Average α_E values for NRUS measurements on separate days, using PZT and EM excitation techniques. Each point on the plot is an average of 10 back-to-back NRUS measurements, but no two sets of 10 were done on the same day. The solid lines are the mean values and the dotted lines are one standard deviation above and below the mean.

3.2 NRUS measurements on different days

When NRUS measurements are taken on different days, the α_E values are much less consistent. Fig. 3.2 shows averages of sets of 10 back-to-back NRUS measurements (just like those described in section 3.1) where each set was done on a separate day, and this plot shows two interesting phenomena. First, there is an absolute error between the EM and PZT techniques; the mean value of α_E for the PZT technique is 5400, while the mean for the EM technique is 30% higher at 7200. Second, there are random errors in measurements for both EM and PZT techniques, with RSTD's of 8.5% for EM excitation and 14.8% for PZT excitation (6.3% higher).

In order to determine whether the random errors are due to the type of sample used or due to the excitation technique employed, NRUS measurements were conducted on a sample of 304 stainless

steel damaged with stress corrosion cracking, using the PZT excitation technique, to see if it would show the same random error in α_E values as Berea sandstone. This sample corresponds to the sample exposed to hot magnesium chloride for 20 days that was included in the recent studies by Hogg *et al.* [5] and Young *et al.* [28].The RSTD for 10 individual NRUS measurements, all taken on separate days, for the steel sample was 22%; even higher than for the sandstone, which shows that high random error is not limited to NRUS on sandstone.

3.3 Coil heating

During an NRUS measurement using the EM excitation technique, the coil generates heat and raises the temperature of the sample by as much as 4°C. Fig. 3.3 shows photographs from a FLIR E60 thermal camera during NRUS measurements using EM and PZT excitation techniques. The coil is seen to heat up the end of the sandstone sample more than the rest of the sample. Tests were conducted to determine whether this heating caused the absolute error in α_E between the PZT and EM excitation techniques. Values of α_E were compared for NRUS measurements using PZT excitation, EM excitation, and PZT excitation while simultaneously driving current through the coil to heat the sample (the electromagnet was moved away from the sample for these measurements). It was hypothesized that if heat from the coil caused the absolute error, the PZT excitation technique with coil heating would measure a mean value of α_E close to the mean value for EM excitation. Instead, the PZT excitation with coil heating measurements gave a mean α_E value of 5100, which is within half a standard deviation of the mean α_E for PZT excitation measurements (5400), but more than three standard deviations away from the mean α_E for EM excitation measurements (7200), suggesting that the coil heating is not the cause of the absolute error.

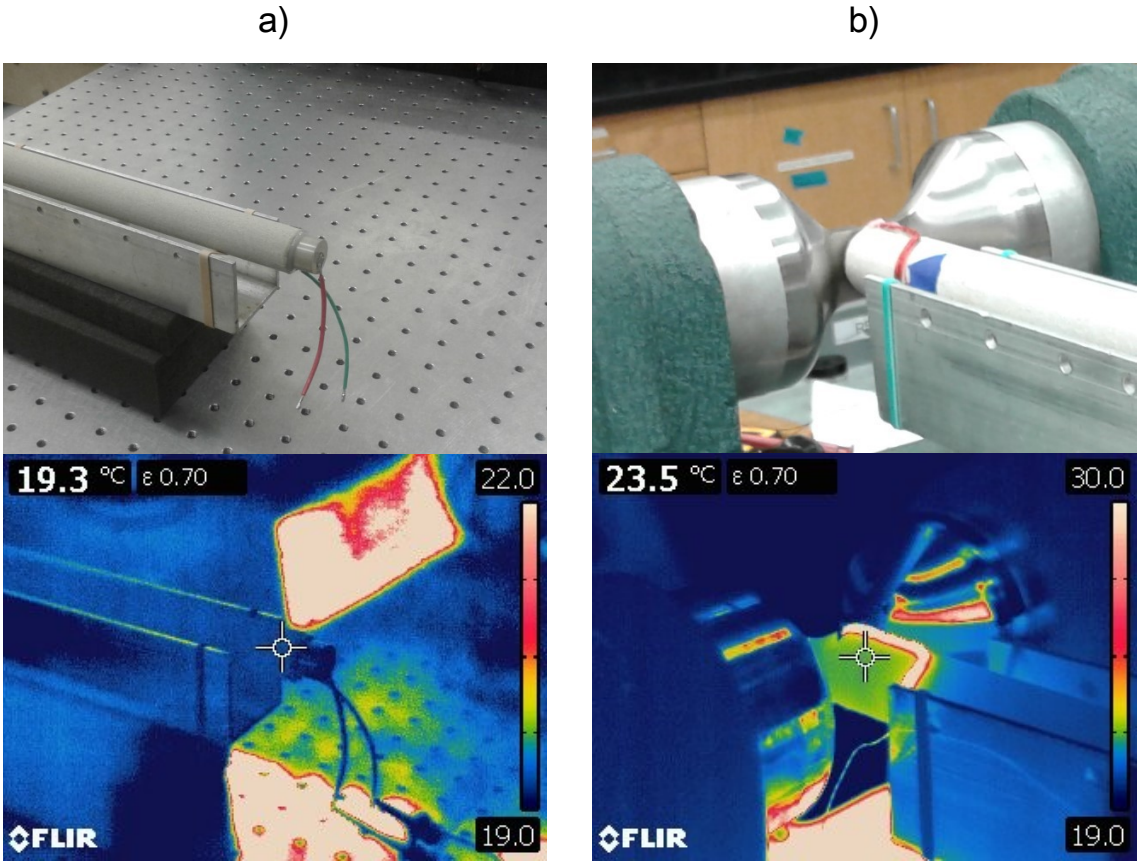

Figure 3.3 Photographs from a thermal camera during NRUS measurements using (a) PZT and (b) EM excitation techniques. The PZT transducer does not generate any noticeable amount of heat, but the coil raises the temperature at the end of the sandstone sample by as much as 4°C.

3.4 Humidity and temperature effects

For the NRUS measurements done on separate days, the room temperature and humidity were recorded to see how they affected the measured α_E values. Plots of the correlation of α_E with humidity and temperature are in Fig. 3.4. For both EM and PZT measurements on the sandstone sample, α_E did not correlate with temperature (the correlation coefficient was 25.5% for the PZT technique and 32.9% for the EM technique), but it did correlate with humidity, with correlation coefficients of 92.1% for the PZT technique and 95.3% for the EM technique. For the steel sample,

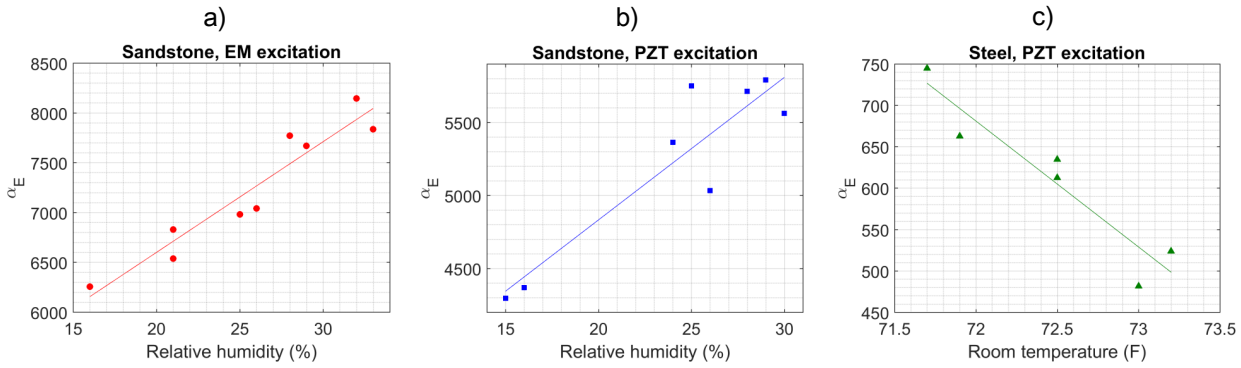

Figure 3.4 Correlation between values of the nonlinearity parameter, α_E, and changing room effects for NRUS measurements on separate days. Plots (a) and (b) show the correlation between α_E and humidity for the sandstone sample, while plot (c) shows the correlation between α_E and temperature for a damaged 304 stainless steel sample.

α_E did not correlate with humidity (the correlation coefficient was 38.3%), but it did correlate with room temperature, with a correlation coefficient of 94%. This suggests that the random errors observed in Fig. 3.2 and in NRUS measurements in general may be due to changing humidity and temperature conditions.

Chapter 4

Conclusions

This thesis has studied the use of the electromagnetic (EM) excitation technique in comparison to the use of the piezoelectric excitation technique using a lead zirconate titanate (PZT) transducer, to extract the nonlinear elastic parameter, α_E. Resonant ultrasound spectroscopy (RUS) and nonlinear resonant ultrasound spectroscopy (NRUS) measurements were conducted on a Berea sandstone sample using the EM excitation technique. NRUS measurements were also conducted using the PZT excitation technique. The EM excitation technique is convenient and capable of exciting longitudinal, torsional, and bending vibrations independently in a rod sample. The EM excitation technique may also be used to conduct NRUS measurements. However, nonlinearity parameter, α_E, measurements obtained using this technique do not agree with α_E values obtained using the traditional PZT excitation technique. An absolute error between values of α_E obtained with the EM and PZT excitation techniques of 30% was observed (with the EM excitation yielding higher values). Random errors between measurements taken on separate days were shown to correlate with humidity or temperature depending on the type of sample used. It is not clear what causes the absolute error, but it is apparently not caused by heat generated by the coil. The random error is apparently caused by changing room conditions: humidity for the sandstone sample, and temperature for a steel sample.

Appendix A

Background Information

A piezoelectric is a material that expands or contracts in one direction when a voltage is applied across it.

A more well-known resonance technique is Resonant Ultrasound Spectroscopy (RUS), which measures the elastic properties of a material by measuring the acoustic resonance frequencies. For a sample with precisely known geometry, the normal resonance modes are known, and its resonance frequencies can be measured and fitted to a theoretical model to extract properties like Young's modulus—also called the modulus of elasticity—and the shear modulus. Fig. A.1 is an example of a RUS measurement, showing the first five resonance frequencies of a sandstone rod. When we want to know the nonlinearity, we use nonlinear resonant ultrasound spectroscopy (NRUS), where we measure how the elastic properties change with vibration amplitude, so we can use just one of the resonance peaks.

NRUS uses similar principles to RUS, but instead of calculating the elastic moduli, we measure the amplitude dependence of the elastic moduli. NRUS involves measuring amplitude-dependent shifts in resonance peaks. It is done by measuring one of the resonance peaks, usually the fundamental, repeatedly at increasing excitation amplitudes (see Fig. A.2). A linear material will show no change in the resonance frequency when the amplitude is changed, but for a damaged material

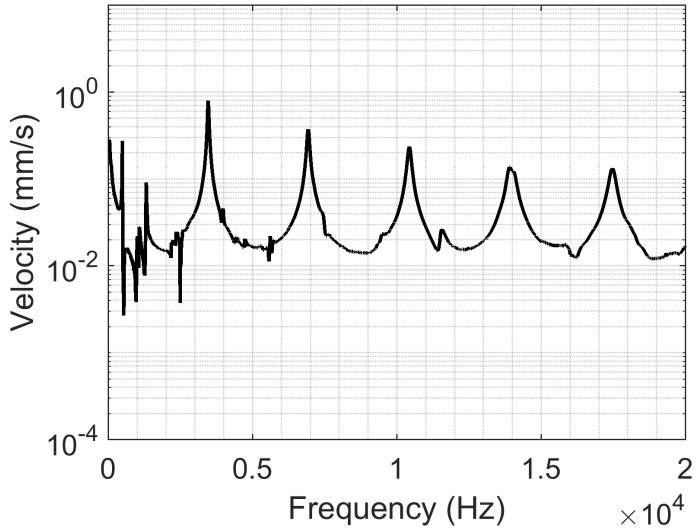

Figure A.1 RUS measurement of a sandstone rod sample, showing the first 5 longitudinal resonance modes.

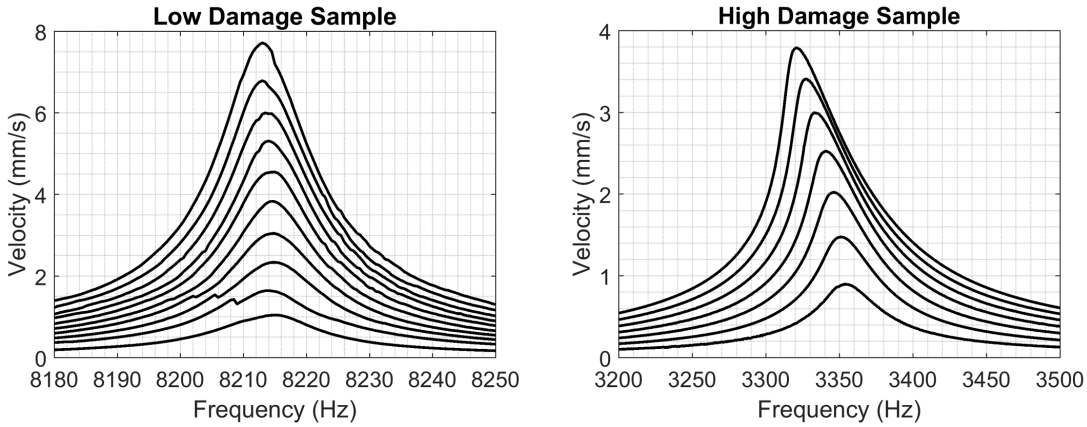

Figure A.2 Amplitude-dependent resonance peak shifting is an indication of damage inside a sample.

the resonance frequency will shift as the amplitude increases. This shift in resonance frequency corresponds to a change in the Young's modulus that depends on the strain in the material, following the relationship $E = E_0(1 - \alpha_E \varepsilon_{max})$. The parameter α_E indicates the degree of nonlinearity in the material.

Future work in this area should be directed toward isolating the differences between the PZT

and EM excitation techniques, verifying the statistical variability of NRUS measurements with different experimental setups, and determining the effect of slow dynamics. This work was not able to identify the cause of the absolute error between techniques, and it will be important to know why they give different results in order to know which technique, if either, is more reliable. More studies on slow dynamics would be helpful in determining what effect slow dynamics has on the measurements, and in which cases it is a significant source of error.

Bibliography

[1] R. A. Guyer and P. A. Johnson, "Nonlinear Mesoscopic Elasticity: Evidence for a New Class of Materials," Phys Today **52,** 30–36 (1999).

[2] J. A. Ten Cate and P. A. Johnson, "Nonlinear resonant ultrasound spectroscopy: Assessing global damage," in *Nonlinear Acoustic Techniques for Nondestructive Evaluation*, 1st ed., T. Kundu, ed., (Springer and Acoustical Society of America, 2018), Chap. 2, pp. 89–101.

[3] S. Haupert, G. Renaud, J. Riviere, M. Talmant, P. A. Johnson, and P. Laugier, "High-accuracy acoustic detection of nonclassical component of material nonlinearity," J. Acoust. Soc. Am. **130,** 2654–2661 (2011).

[4] K. V. D. Abeele, P. Y. L. Bas, B. V. Damme, and T. Katkowski, "Quantification of material nonlinearity in relation to microdamage density using nonlinear reverberation spectroscopy: Experimental and theoretical study," J. Acoust. Soc. Am. **126,** 963–972 (2009).

[5] S. M. Hogg, B. E. Anderson, P.-Y. L. Bas, and M. C. Remilieux, "Nonlinear resonant ultrasound spectroscopy of stress corrosion cracking in stainless steel rods," NDT E Int **102,** 194–198 (2019).

[6] D. A. Van, J. Carmeliet, P. A. Johnson, and B. Zinszner, "Influence of water saturation on the nonlinear elastic mesoscopic response in Earth materials and the implications to the

mechanism of nonlinearity," Journal of Geophysical Research: Solid Earth **107,** ECV4–1–ECV4–11 (2002).

[7] J. Chen, J.-Y. Kim, K. E. Kurtis, and L. J. Jacobs, "Theoretical and experimental study of the nonlinear resonance vibration of cementitious materials with an application to damage characterization," J. Acoust. Soc. Am. **130,** 2728–2737 (2011).

[8] P. Johnson, J. Ten Cate, R. Guyer, and K. V. D. Abeele, "Resonant nonlinear ultrasound spectroscopy," US Patent 6330827, 18 Dec 2001 .

[9] P. Johnson, B. Zinszner, and P. Rasolofasaon, "Resonance and elastic nonlinear phenomena in rock," J. Geophys. Res. **101,** 11553–11564 (1996).

[10] D. Pasqualini, K. Heitmann, J. Ten Cate, S. Habib, D. Higdon, and P. Johnson, "Nonequilibrium and nonlinear dynamics in Berea and Fontainebleau sandstones: Low-strain regime," J. Geophys. Res. **112,** 1–16 (2007).

[11] M. C. Remillieux, R. A. Guyer, C. Payan, and T. J. Ulrich, "Decoupling Nonclassical Nonlinear Behavior of Elastic Wave Types," Phys. Rev. Lett. **116,** 115501 (2016).

[12] S. L. Garrett, "Resonant acoustic determination of elastic moduli," J. Acoust. Soc. Am. **88,** 210–221 (1990).

[13] M. C. Remillieux, B. E. Anderson, T. Ulrich, P.-Y. L. Bas, M. R. Haberman, and J. Zhu, "Review of Air-Coupled Transduction for Nondestructive Testing and Evaluation," In , pp. 36–45 (2014).

[14] T. Alvarez-Arenas, "Acoustic impedance matching of piezoelectric transducers to the air," IEEE Trans Ultrason Ferroelectr Freq Control **51,** 624–633 (2004).

[15] D. W. Schindel, D. A. Hutchins, and W. A. Grandia, "Capacitive and piezoelectric air-coupled transducers for resonant ultrasonic inspection," Ultrasonics **34,** 621–627 (1996).

[16] F. Akasheh, T. Myers, J. D. Fraser, S. Bose, and A. Bandyopadhyay, "Development of piezoelectric micromachined ultrasonic transducers," Sens Actuators A Phys **111,** 275–287 (2004).

[17] B. T. Khuri-Yakub and O. Oralkan, "Capacitive micromachined ultrasonic transducers for medical imaging and therapy," J Micromech Microeng **21,** 054004 (2011).

[18] J. Viertl, "Frequency-Spectrum of Laser-Generated Ultrasonic-Waves," J. Appl. Phys. **51,** 805–807 (1980).

[19] P.-Y. L. Bas, T. J. Ulrich, B. E. Anderson, and J. J. Esplin, "A high amplitude, time reversal acoustic non-contact excitation (trance)," J. Acoust. Soc. Am. **134,** EL52–EL56 (2013).

[20] X. Dai, J. Zhu, and M. R. Haberman, "A focused electric spark source for non-contact stress wave excitation in solids," J. Acoust. Soc. Am. **134,** EL513–EL519 (2013).

[21] B. W. Drinkwater and P. D. Wilcox, "Ultrasonic arrays for non-destructive evaluation: A review," NDT E Int **39,** 525–541 (2006).

[22] L. E. Kinsler, A. R. Frey, A. B. Coppens, and J. V. Sanders, *Fundamentals of Acoustics*, 4th ed. (Wiley, New York, 2000), pp. 68–87.

[23] S. L. Garrett, *Understanding Acoustics* (Springer and ASA Press, New York, 2017), Chap. 5, pp. 279–305.

[24] T. D. Rossing and D. A. Russell, "Laboratory observation of elastic waves in solids," Am. J. Phys. **58,** 1153–1162 (1990).

[25] B. E. Anderson and W. D. Peterson, "The song of the singing rod," J. Acoust. Soc. Am. **131,** 2435–2443 (2012).

[26] S. K. Chakrapani and D. J. Barnard, "Determination of acoustic nonlinearity parameter (β) using nonlinear resonance ultrasound spectroscopy: Theory and experiment," J. Acoust. Soc. Am. **141,** 919–928 (2017).

[27] J. A. Ten Cate and T. J. Shankland, "Slow dynamics in the nonlinear elastic response of Berea sandstone," Geophys Res Lett **23,** 3019–3022 (1996).

[28] S. M. Young, B. E. Anderson, S. M. Hogg, P.-Y. L. Bas, and M. C. Remillieux, "Nonlinearity from stress corrosion cracking as a function of chloride exposure time using the time reversed elastic nonlinearity diagnostic," J. Acoust. Soc. Am. **145,** 382–391 (2019).

Index